PHYSICS AND CHEMISTRY OF SOLID STATE
V. 24, No. 1 (2023) pp. 92-101
Section: Physics
DOI: 10.15330/pcss.24.1.92-101

Vasyl Stefanyk Precarpathian National University

ФІЗИКА І ХІМІЯ ТВЕРДОГО ТІЛА
Т. 24, № 1 (2023) С. 92-101
Фізико-математичні науки

PACS: 71.15.Mb, 74.20.Pq, 74.25.Gz ISSN 1729-4428

A.I. Kashuba

Influence of metal atom substitution on the electronic and optical properties of solid-state $Cd_{0.75}X_{0.25}Te$ (X= Cu, Ag and Au) solutions

Department of General Physics, Lviv Polytechnic National University, Lviv, Ukraine, andrii.i.kashuba@lpnu.ua

The solid-state $Cd_{0.75}X_{0.25}Te$ (*X*= Cu, Ag, and Au) solutions crystallize in the cubic structure and are studied in the framework of density functional theory. The theoretical first-principle calculations of the electronic band structure, density of states, and refractive index of solid-state $Cd_{0.75}X_{0.25}Te$ (*X*= Cu, Ag, and Au) solutions are estimated by the generalized gradient approximation (GGA). A Perdew–Burke–Ernzerhof functional (PBE) was utilized. Formation energy is calculated based on the results of the total energy of the study samples. The effective mass of the electrons and holes was calculated based on the electronic band structure. The influence of atom substitution on electron conductivity and mobility is discussed. To study the optical properties was use a complex dielectric function ε(ħω). The spectral behaviour of the refractive index was calculated based on the dielectric function.

Keywords: density functional theory, electron band structure, formation energy, effective mass, density of state, refractive index.

Received 10 December 2022; Accepted 6 March 2023.

Introduction

Cadmium chalcogenides (CdY, with Y= S, Se and Te) represent the $A^{II}B^{VI}$ group of crystalline materials that reveal a semiconducting behaviour. These materials embrace large and important research fields because of their wide application potential in various fields of optoelectronic devices [1]. CdTe semiconductor has proven to be a leading compound for manufacturing cost-effective second-generation photovoltaic devices [1]. Cadmium telluride is having a direct band gap with an energy of ~1.45 eV and a high absorbance (above $10^5 cm^{-1}$) [2–4]. This makes it an excellent light-absorbing layer for solar cells. Now, for building solar cells use the low dimensions of the photovoltaic cells. In particular, it's a thin film. Usually, CdTe is deposited on glass, quarts, mica, silicon or many other substrates. But it can also be deposited on substrates like metal foil or polymer sheets [5–7]. Also, Ref. [7] quoted that the formation of a low resistive contact on the CdTe surface is one of the most critical issues for the fabrication of a highly efficient CdTe thin film solar cell. Schottky energy barrier is higher than ~0.4 eV, and is formed at the CdTe/metal back contact interface [7–9]. Schottky barrier can be efficiently lowed by doping the CdTe surface using a thin layer of Cu [6, 7, 9]. Cu can diffuse from the back contact into the CdTe thin film. As a result, Cu cans entry in CdTe as a doping element, which is a donor. Also, copper can substitute cadmium atoms or free position of Cd vacancy. In literature found many experimental works with studies of Cu and/or Ag doping/substitution in CdTe [10–17]. About identification of Cu and Ag acceptor levels in CdTe was a study in Ref. [18].

A new step in studies of low-dimension systems is quantum dots (QDs) or nanocrystals (NCs) [19, 20]. Also, QDs based on CdTe have potential applications in novel light emitters, next-generation solar cells, sensing, and biomedical diagnostics [19]. This research branch has a perspective using doped QDs, such as CdTe:Au [19].

In the present work, the electronic band structure, formation energy, density of states and refractive index of the solid-state $Cd_{0.75}X_{0.25}Te$ (*X*= Cu, Ag and Au) solutions have been calculated for the first time. In the literature was founded information about studies of physical properties of the CdTe with Cr-doped [21–23], Sn-doped [24], V and P-

doped [25], Cu-doped [26], V-dopes [23, 27], As and P-doped [28], Cl-doped [29]. In the case of substitution of Cd atom in CdTe usually using atoms of Mn [30, 31], Ti [32], Zn [33], et al. Only diffusion of Cd vacancies and interstitials of Cd, Cu, Ag, Au and Mo in CdTe was studied in Ref. [34].

The paper is organized as follows. The next section introduces the calculation techniques used. The first subsection in the second section reports the main results of the structure analysis of solid-state $Cd_{0.75}X_{0.25}Te$ (X= Cu, Ag and Au) solutions. *Ab initio* calculations of the formation energy of solid-state $Cd_{0.75}X_{0.25}Te$ (X= Cu, Ag and Au) solutions are elucidated in the second subsection. The third subsection in the second section is the study of the electronic band structure of the solid solutions. The density of states and refractive index of the solid-state $Cd_{0.75}X_{0.25}Te$ (X= Cu, Ag and Au) solutions are elucidated in the fourth and five subsections, respectively. Finally, the conclusions are drawn in the last section.

I. Methods of calculation

In preview work [35], was reported about electron, phonon, optical and thermodynamic properties of the CdTe crystal. In the present work, the electronic energy spectra of the solid-state $Cd_{0.75}X_{0.25}Te$ (X= Cu, Ag and Au) solutions have been calculated for the first time. The theoretical calculations were performed within the framework of the density functional theory (DFT). To calculate the properties of single-crystalline $Cd_{0.75}X_{0.25}Te$, a crystalline lattice with the basal parameters given below in Table 1 was used. To describe the exchange-correlation energy of the electronic subsystem, we used a functional taken in the approximation of generalized gradient (GGA) and Perdew –Burke–Ernzerhof (PBEsol) parameterization [36]. Ultrasoft Vanderbilt's pseudopotentials [37] served as ionic potentials.

In our calculations, the value $E_{cut\text{-}off}$= 880 eV was taken for the cutting-off energy of the plane waves (this energy corresponded to the minimum value of the total energy). The convergence of the total energy was about 5×10^{-6} eV/atom. Integration over the Brillouin zone (BZ) was performed on a 2×2×2 grid of k points, using a Monkhorst–Pack scheme [38]. At the initial stage of our calculations, we optimized a starting CdTe structure for the case of 3×3×3 supercell (see Ref. [35]). The atomic coordinates and the unit-cell parameters were optimized following a Broyden–Fletcher–Goldfarb–Shanno technique. Optimization was continued until the forces acting on atoms became less than 0.01 eV/Å, the maximum displacement less than 5.0×10^{-4} Å, and the mechanical stresses in the cell less than 0.02 GPa. The energy band diagram was constructed using the points X(0.5, 0, 0.5), R(0.5, 0.5, 0.5), M(0.5, 0.5, 0) and Γ(0,0,0) of the Brillouin zone in the reciprocal space (see Fig. 1).

The $Cd_{0.75}X_{0.25}Te$ (X= Cu, Ag and Au) samples were modelled as follows. First formed a 3×3×3 supercell of the initial compound, CdTe, based on its already optimized structure. The next stage was the theoretical construction of solid-state $Cd_{0.75}X_{0.25}Te$ (X= Cu, Ag and Au) solutions. In the optimization structure CdTe, Cd atoms were gradually replaced by X (X= Cu, Ag and Au). For such substitution, the crystal structure of optimization structure CdTe was changed on a triclinic with symmetry $P1$. Finally, structures of $Cd_{0.75}X_{0.25}Te$ (X= Cu, Ag and Au) were optimization with finding crystal structure. Obtained of $Cd_{0.75}Ag_{0.25}Te$ structure is drawn in figure 2 for visualization. Optimization lattice parameters and bulk modules (B) are listed in Table 1 (see section 2.1).

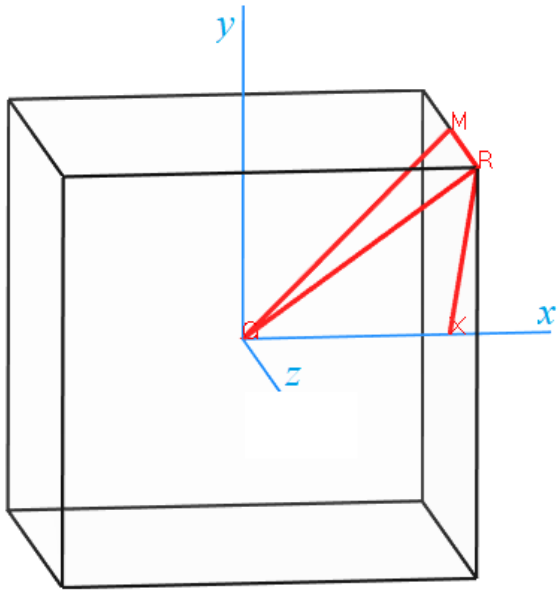

Fig. 1. BZ of cubic $Cd_{0.75}X_{0.25}Te$ (X= Cu, Ag and Au) crystal.

Table 1.
Structure parameters of $Cd_{0.75}X_{0.25}Te$ (X= Cu, Ag and Au) crystals

Sample	a, Å	V, Å^3	B, GPa
$Cd_{0.75}Cu_{0.25}Te$	6.39181	261.14	46.3
$Cd_{0.75}Ag_{0.25}Te$	6.45826	269.37	54.9
$Cd_{0.75}Au_{0.25}Te$	6.46845	270.65	43.3

II. Results and Discussion

2.1. Crystal structure of solid-state $Cd_{0.75}X_{0.25}Te$ (X= Cu, Ag and Au) solutions

The X-ray diffraction data (XRD) of solid-state $Cd_{0.75}X_{0.25}Te$ (X= Cu, Ag and Au) solutions was been simulation and shown in figure 3. Theoretical XRD of CdTe crystals with cubic structure is given for comparison.

The XRD (see Fig. 3(a)) show that all samples have one intense reflection peak of approximately between 30°–30.4°. If compared these data with the cubic CdTe, we can see that the main peak shifts to a higher region. Also, the maximum shifting of the main peak is obtained for sample $Cd_{0.75}Cu_{0.25}Te$ (see Fig. 3(b)).

As result, solid-state $Cd_{0.75}X_{0.25}Te$ (X= Cu, Ag and Au) solutions crystallize in a cubic structure, with the unit-cell dimensions for different samples and atoms position listed in Table 1 and 2, respectively.

In Fig. 4, the structure parameters and bulk modules of the solid-state $Cd_{0.75}X_{0.25}Te$ (X= Cu, Ag and Au) solutions

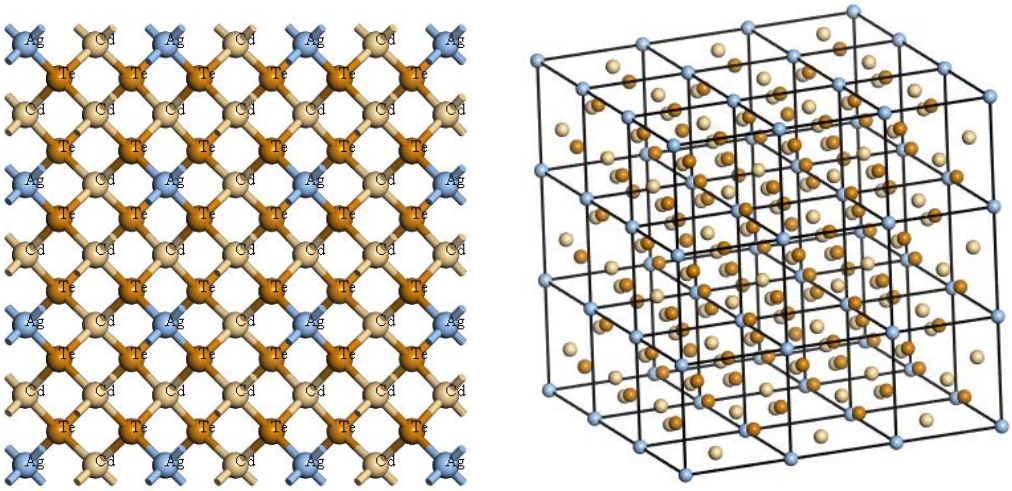

a *b*

Fig. 2. Crystal structure (*a*) in (1 1 0) plane and 3×3×3 supercell (*b*) of $Cd_{0.75}Ag_{0.25}Te$ crystal.

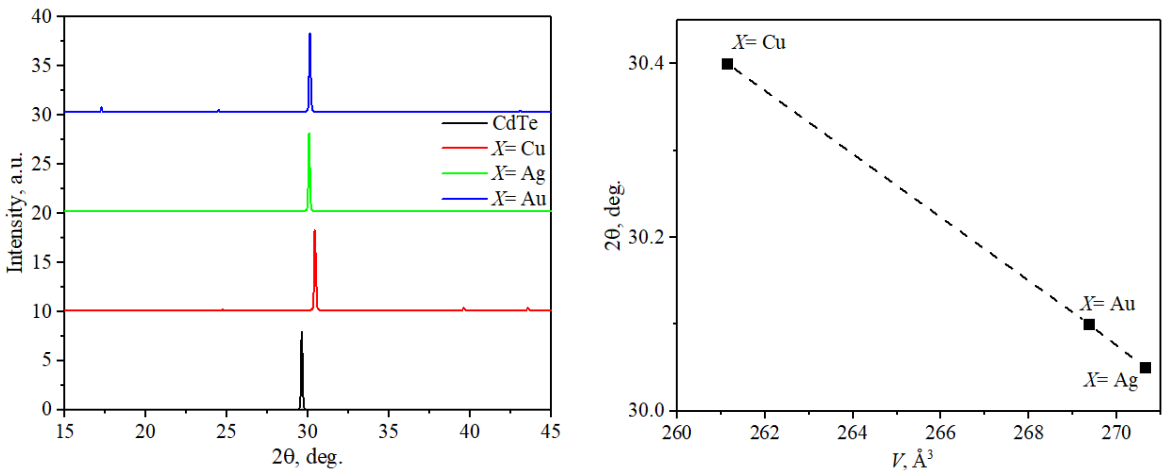

a *b*

Fig. 3. Theoretical XRD (*a*) of solid-state $Cd_{0.75}X_{0.25}Te$ (*X*= Cu, Ag and Au) solutions (see information in legend).

Table 2.

Atoms position of $Cd_{0.75}X_{0.25}Te$ (*X*= Cu, Ag and Au) crystals

Element	Atom Number	*x/a*	*y/b*	*z/c*
X= Cu/Ag/Au	1	0.0	0.0	0.0
Cd	1	0.0	0.5	0.5
Cd	2	0.5	0.0	0.5
Cd	3	0.5	0.5	0.0
Te	1	0.241779	0.241779	0.241779
Te	2	-0.241779	-0.241779	0.241779
Te	3	-0.241779	0.241779	-0.241779
Te	4	0.241779	-0.241779	-0.241779

are shown as a function of the atom radius *X* (*X*= Cu, Ag and Au). This analysis is show that lattice parameters (*a*) and volume cell (*V*) linearly increase with increasing atom radius of substitutions element. But, the bulk module is shown a maximum value, 54.9 GPa, for sample $Cd_{0.7}Ag_{0.25}Te$. Also, the minimum value, 43.3 GPa, was obtained for $Cd_{0.7}Au_{0.25}Te$ and not much higher (46.3 GPa) for $Cd_{0.7}Cu_{0.25}Te$. If compared these data with the data obtained from a calculation using the same method for CdTe (45.13 GPa [35]), we can see that the solid-state $Cd_{0.75}Cu_{0.25}Te$ solution shows a much close value.

2.2 Formation energy of solid-state $Cd_{0.75}X_{0.25}Te$ (*X*= Cu, Ag and Au) solutions

For solid-state $Cd_{0.75}X_{0.25}Te$ solutions was considered only one position of locating *X* (*X*= Cu, Ag and Au) atoms in the structure of 'parent' CdTe (see information in Table 2). The formation energy of solid-state $Cd_{0.75}X_{0.25}Te$ solutions, when there is a substitution of Cd atom by *X* (*X*= Cu, Ag and Au) atom is considered, is estimated pursuant to the following equation:

$$E_f = E_{SSS} + E_{Cd} - E_{CdTe} - E_X, \quad (1)$$

where E_{SSS} correspond to the total energies of the solid-state $Cd_{0.75}X_{0.25}Te$ (X= Cu, Ag and Au) solutions (SSS denoted as a solid-state solution), E_{CdTe} is the total energies of the 'parent' CdTe compound and E_X and E_{Cd} are total energies of free X (X= Cu, Ag and Au) and Cd atoms, respectively. The optimized free Cd and X (X= Cu, Ag and Au) atoms energies were calculated in the same unit cell as all samples. Positive formation energy denotes the replacement process is endothermic, while negative formation energy denotes the replacement process is exothermic [39]. Formation energy was calculated for all solid-state $Cd_{0.75}X_{0.25}Te$ (X= Cu, Ag and Au) solutions are presented in Table 3. As seen from Table 3, such position of replacements (see Table 2) produces an endothermic process for all studied samples. All studies samples obtained large values of formation energy. Also, high formation energy (1.1–15.0 eV) was reported for cubic SiC samples with different point defects [40]. Defective formation of atomic vacancy in solid-state $Cd_{0.75}X_{0.25}Te$ (X= Cu, Ag and Au) solutions are not studied in this work.

Table 3.

Formation energy of $Cd_{0.75}Me_{0.25}Te$ (Me= Cu, Ag and Au) crystals

Sample	$E_{tot}^{SSS}/E_{tot}^{CdTe}$	E_f, eV
$Cd_{0.75}Cu_{0.25}Te$	0.997	11.05
$Cd_{0.75}Ag_{0.25}Te$	1.491	11.86
$Cd_{0.75}Au_{0.25}Te$	0.949	11.22

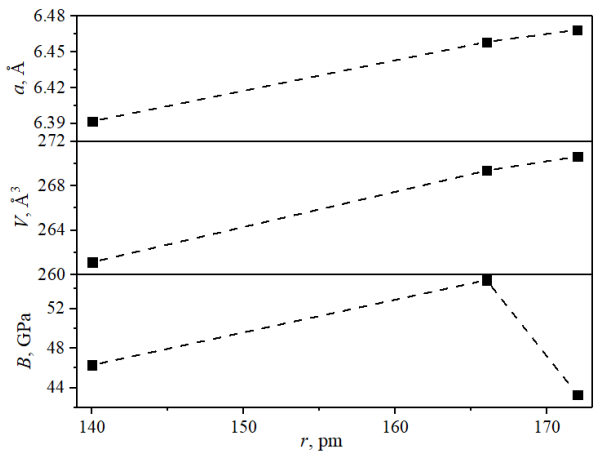

Fig. 4. Crystal cell parameters and bulk modules of solid-state $Cd_{0.75}X_{0.25}Te$ (X= Cu, Ag and Au) solutions as function atom radius of substitutions element.

2.3 Electron band energy structure of solid-state $Cd_{0.75}X_{0.25}Te$ (X= Cu, Ag and Au) solutions

In Fig. 5, the full energy band diagrams of the solid-state $Cd_{0.75}X_{0.25}Te$ (X= Cu, Ag and Au) solutions are shown along the highly symmetric lines of the BZ. The energy in this case is counted from the Fermi level. Analysis of the results of theoretical calculations of the energy band spectrum shows that the smallest optical band gap is localized in the center of the BZ (the point Γ). This means that the crystal is characterized by a direct energy optical band gap.

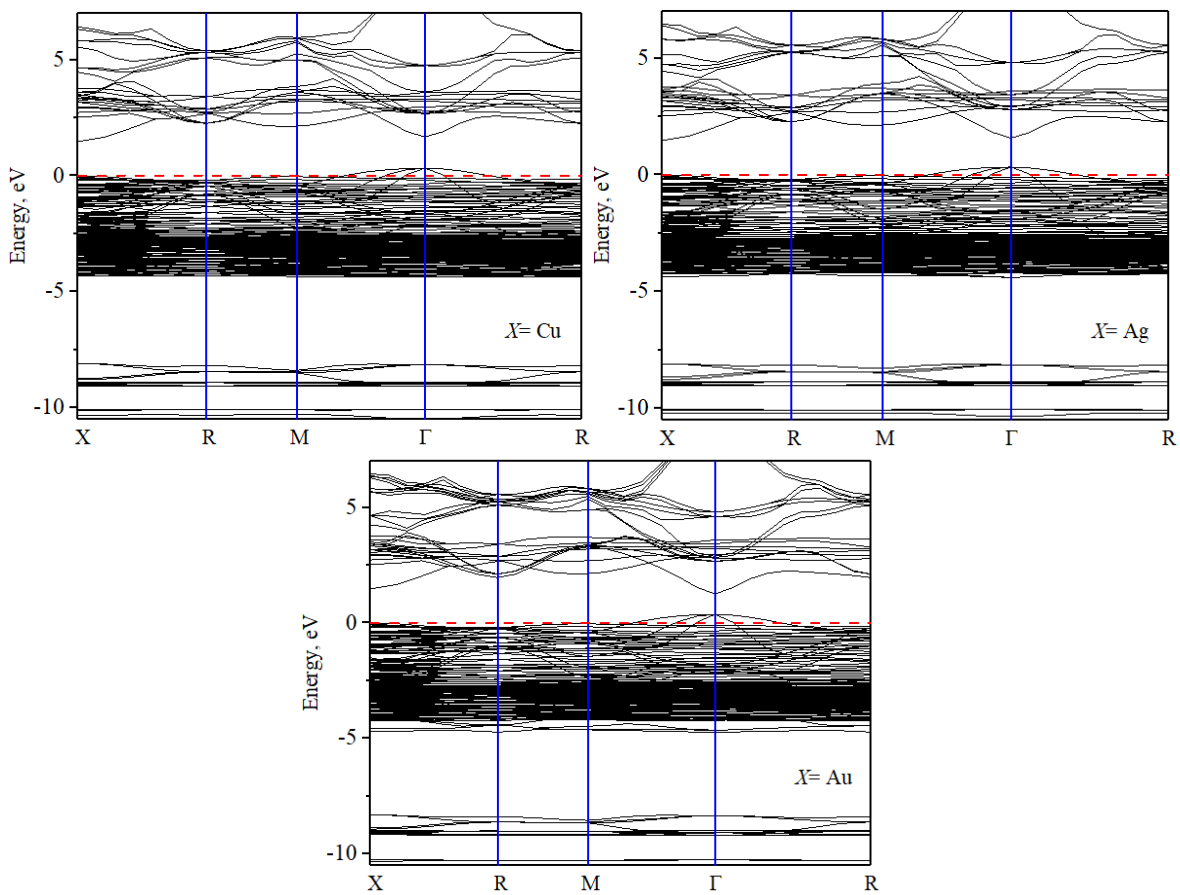

Fig. 5. Electron band energy structure of solid-state $Cd_{0.75}X_{0.25}Te$ (X= Cu, Ag and Au) solutions (see information on legend). The red line corresponded to the position of the Fermi level.

Position of the higher energy level of the valence band (E_v^{top}), the lower energy level of the conduction band (E_c^{bot}), and their difference (corresponded to optical band gap; E_c^{bot}–E_v^{top}) at Γ-point of k-space as a function of the atomic number (Z) of X (X= Cu, Ag and Au) for the solid-state $Cd_{0.75}X_{0.25}Te$ (X= Cu, Ag and Au) solutions are presented on figure 6. As we can see from Fig. 6, the Fermi level is shifted to the valence band on 0.32–0.37 eV. Assumed to be this solid-state $Cd_{0.75}X_{0.25}Te$ (X= Cu, Ag and Au) solutions are a degenerate semiconductor. But, this result must be approved by other experimental studies. Also, obtained decrease tendency of optical band gap with increasing atomic number. Such behaviour Fermi level was observed in the defection sample CdTe and with substitution of Te on Cl [29].

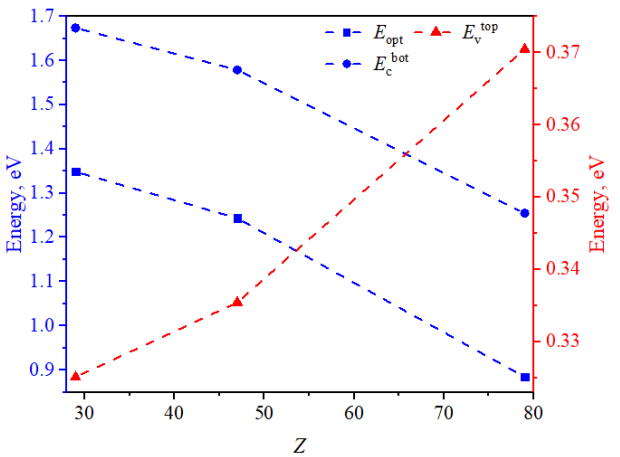

Fig. 6. Position of the higher energy level of the valence band (E_v^{top}), the lower energy level of the conduction band (E_c^{bot}), and their difference (corresponded to optical band gap; E_c^{bot}–E_v^{top}) for the solid-state $Cd_{0.75}X_{0.25}Te$ (X= Cu, Ag and Au) solutions as a function of the atomic number, obtained from *ab initio* calculations.

2.4 Dispersion of the electron band energy structure of solid-state $Cd_{0.75}X_{0.25}Te$ (X= Cu, Ag and Au) solutions

In addition, one can see a clear anisotropy difference E(k) between the valence and conduction bands (see Fig. 5). The valence complex top is flatter, which is explained by the fact that holes are less mobile than electrons. This behaviour is caused by the inverse relationship between the effective mass (m^*) of the electron(m_e^*)/hole(m_h^*) and the spread E(k) of energy levels [41]:

$$\frac{1}{m^*} = \frac{4\cdot\pi^2}{h^2}\frac{d^2E(k)}{dk^2}, \qquad (2)$$

where h is the Planck constant, and E(k) is the dependence of the band energy E on the electron wave vector k. As result, we can see that the maximum dispersion of valence and conduction bands was observed for Γ→R and Γ→M direction.

Information on the quantitative value of m^* for a material is important because this value determines the dynamics of electron conductivity in it and therefore is significant for the corresponding practical applications. The effective masses of electrons and holes in solid-state $Cd_{0.75}X_{0.25}Te$ (X= Cu, Ag and Au) solutions have been calculated by utilizing the Effective Mass Calculator [42]. The calculated effective masses are presented in Table 4 and figure 7. The resultant absolute value of the $|m^*|$ for the conduction band is lower than that for the valence band. Also, we can see that the value of electron (m_e^*) effective mass increases with the atom radius of X element.

Table 4.
Effective mass of the electron (m_e^*) and hole (m_h^*) of $Cd_{0.75}X_{0.25}Te$ (X= Cu, Ag and Au) crystals

Sample	Effective mass	
	m_c/m_0	m_v/m_0
$Cd_{0.75}Cu_{0.25}Te$	0.82	-2.29
$Cd_{0.75}Ag_{0.25}Te$	0.99	-2.44
$Cd_{0.75}Au_{0.25}Te$	0.95	-2.24

In Ref. [43] was reported that the absolute value ($|m^*|$) of electron (m_e^*) and hole (m_h^*) effective mass is $0.096m_0$ and 0.35 m_0. In this study, we obtained the absolute value of the effective mass of the electron and hole value near (0.82–0.92)m_0 and (2.24–2.44)m_0, respectively. This value is much higher than for CdTe. Also, this behaviour will influence the electrical conductivity of solid-state $Cd_{0.75}X_{0.25}Te$ (X= Cu, Ag and Au) solutions. According to the semiconductor theory [41] the specific conductivity σ of a material is dependent on the charged particle's mobility (μ),

$$\sigma = nq\mu, \qquad (3)$$

where q is the particle's charge and n is the charged particle's concentration. The electron mobility μ is associated with an impurity of the i-type may be presented by the following relation [44, 45]:

$$\mu_i = \frac{q\tau_i}{m^*}, \qquad (4)$$

where τ_i is the relaxation time, which is inversely proportional to the ionized impurity concentration n_i

$$\tau_i \infty n_i^{-1} T^{3/2}. \qquad (5)$$

Here T is the thermodynamic temperature. At this time, the electron mobility μ satisfies the following relation:

$$\mu_i \infty \frac{qT^{3/2}}{m^* n_i}. \qquad (6)$$

Analysis of Eq. (6) and (3) shows that the electron mobility and conductivity are higher than hole mobility and conductivity ($|m_h^*|/|m_e^*|>1$) for all studies compound, increases with increasing temperature ($\mu_i \sim T^{3/2}$) and decreases with increasing carrier concentration ($\mu_i \sim n_i^{-1}$).

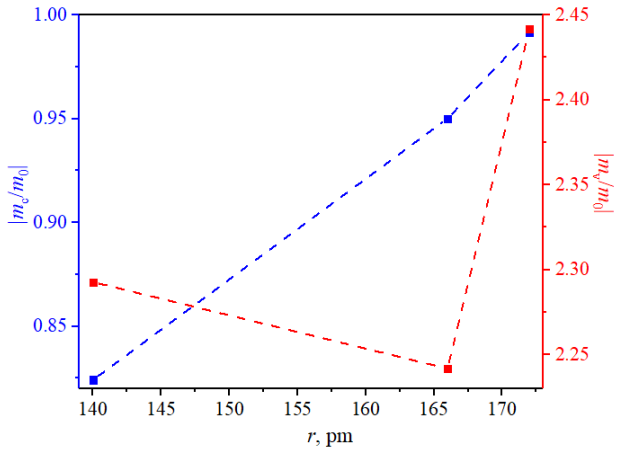

Fig. 7. Effective mass of the electron (m_e*) and hole (m_h*) of solid-state $Cd_{0.75}X_{0.25}Te$ (X= Cu, Ag and Au) solutions as function atom radius of substitutions element.

2.5 Density of states of the solid-state $Cd_{0.75}X_{0.25}Te$ (X= Cu, Ag and Au) solutions

Also, the electron density of states of solid-state $Cd_{0.75}X_{0.25}Te$ (X= Cu, Ag and Au) solutions for obtaining the 'nature' of the band structure are studied. The analysis of the partial contributions of individual levels to the function of the total density of states (Fig. 8) and the partial contributions of individual bands to the electronic density allows us to find the genesis of the valence and conduction bands for solid-state $Cd_{0.75}X_{0.25}Te$ (X= Cu, Ag and Au) solutions.

The lowest band near –10 eV is formed by the *s* states of Te. The following bands dispersed at the energy marker near –9 eV are formed because of the contributions of the *d* states of Cd. Electron bands near 4 eV are formed by the *s*-state of Cd and *X* element, and the *p*-state of Te. The peak of the valence complex is practically formed by the *p* states of Te, with 'contamination' of the *p* states of Cd and *X* elements. But the conduction band bottom is mainly

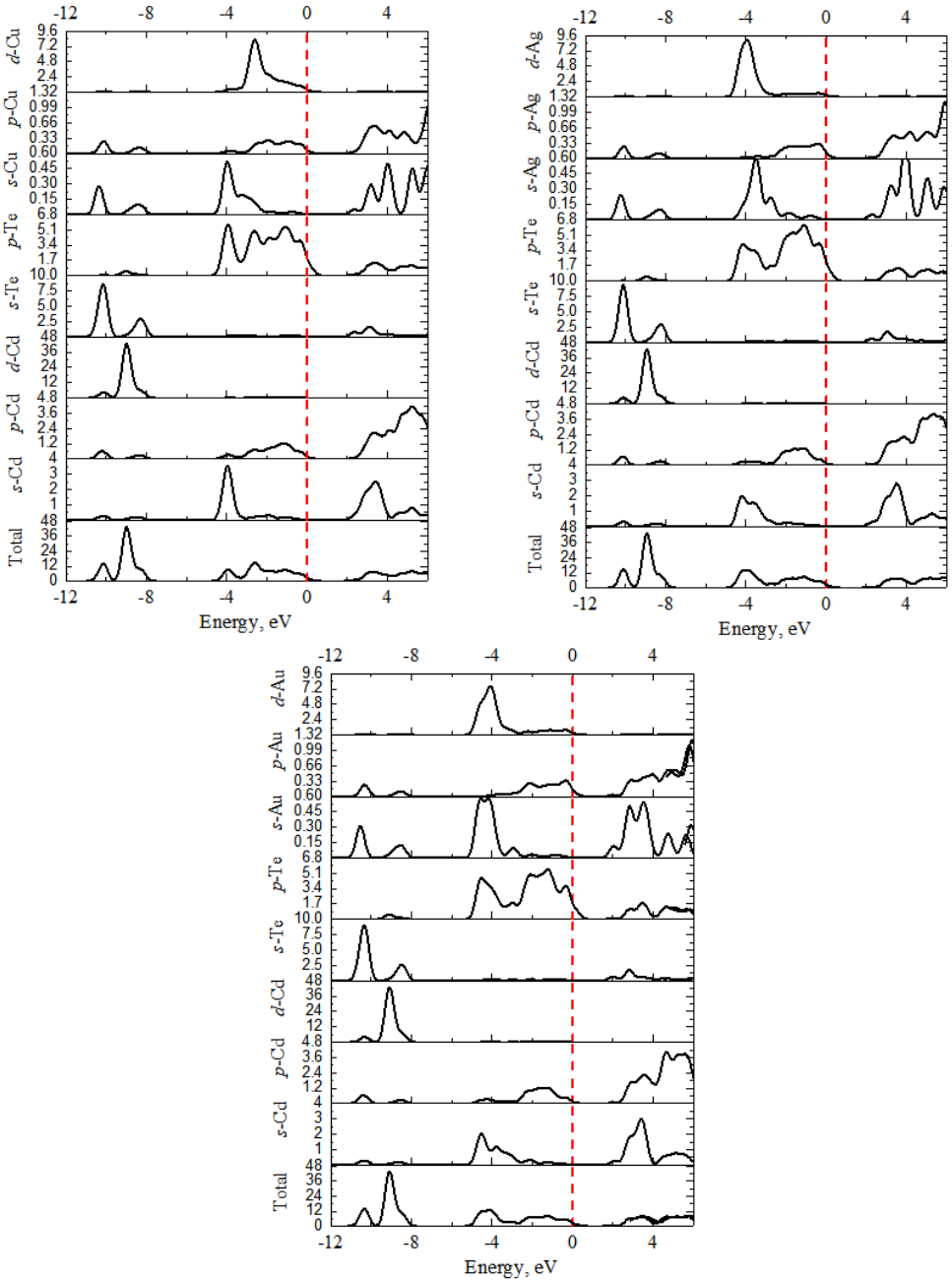

Fig. 8. Partial and total electron density of states of solid-state $Cd_{0.75}X_{0.25}Te$ (X= Cu, Ag and Au) solutions.

formed by the *s*– and *p*– states of the Cd and *X* elements.

2.6 Refractive index of the solid-state $Cd_{0.75}X_{0.25}Te$ (*X*= Cu, Ag and Au) solutions

Finally, in this work are present spectral behaviours of the refractive index. To study the optical properties of solid-state $Cd_{0.75}X_{0.25}Te$ (*X*= Cu, Ag and Au) solutions is use a complex dielectric function $\varepsilon(\hbar\omega)= \varepsilon_1 + i\varepsilon_2$. Its imaginary part can be calculated as

$$\varepsilon_2 = \frac{2e^2\pi}{V\varepsilon_0}\sum_{K,v,c}|\langle\psi_K^c|\hat{u}\cdot r|\psi_K^v\rangle|^2\,\delta(E_K^c - E_K^v - \hbar\omega), \quad (7)$$

while the real part can be obtained from the Kramers–Kronig relation

$$\varepsilon_1 - 1 = \frac{2}{\pi}\int_0^\infty \frac{t\varepsilon_2(t)dt}{t^2-(\hbar\omega)^2}. \quad (8)$$

Using the data obtained for the real and imaginary parts of the dielectric function, one can calculate the spectral dependences of the refractive index *n*:

$$n = \sqrt{\frac{(\varepsilon_1^2+\varepsilon_2^2)^{1/2}+\varepsilon_1}{2}}. \quad (9)$$

Fig. 9(*a*) shows the spectral dependences of the refractive index for solid-state $Cd_{0.75}X_{0.25}Te$ (*X*= Cu, Ag and Au) solutions. Need to be noted that a refractive index below 300 nm are showing practically the same spectral behaviour for all samples. In visible spectral region are obtained three local maximums (see Fig. 9(*b*)). Also, the maximum value of the refractive index (200-2500 nm) for solid-state $Cd_{0.75}X_{0.25}Te$ solutions was obtained for *X*= Cu and Ag near 280 nm, but for *X*= Au near 435 nm.

Analysis of the near infrared spectra (IR) region are showing one broad maximum between 1500 and 1800 nm (see Fig. 9(*a*)). The maximum value of the refractive index in this region is shifting to a higher wavelength region with decreasing atomic number (Au → Cu). The maximum value is obtained for solid-state $Cd_{0.75}Au_{0.25}Te$ solutions and the minimum for $Cd_{0.75}Ag_{0.25}Te$ in this IR region.

Conclusion

The lattice parameters (*a*, *V*) linearly increase with increasing atom radius of substitutions element. The bulk module shows a maximum value for the sample with substitutions atoms Cd on the Ag. Solid-state $Cd_{0.75}Cu_{0.25}Te$ solution shows a much close value to 'pure' CdTe.

First-principle theoretical studies of the electron energy spectrum for the solid-state $Cd_{0.75}X_{0.25}Te$ (*X*= Cu, Ag and Au) solutions have been carried out using the reliable techniques of density functional theory and known approximations. It has been established that the smallest optical band gap is localized at the center of the BZ and should reveal direct optical transitions. The Fermi level is shifted to the valence band on 0.32–0.37 eV for all studies samples. Formation energy was calculated for solid-state $Cd_{0.75}X_{0.25}Te$ (*X*= Cu, Ag and Au) solutions and changed in the range between 11.05 and 11.86 eV. The absolute value of the effective mass of the electron (0.82–0.99m_0) and hole (2.24–2.44m_0) was calculated based on the results of the electronic structure. The electron mobility and conductivity are higher than hole mobility and conductivity ($|m_h^*|/|m_e^*|>1$) for all studied compounds. The biggest value of the electron mobility and conductivity corresponded to $Cd_{0.75}Cu_{0.25}Te$. Based on the electron density of states was obtained that the peak of the valence complex formed by the *p* states of Te, with 'contamination' of the *p* states of Cd and *X* elements. The conduction bottom band is mainly formed by the *s*– and *p*– states of the Cd and *X* elements.

To study the optical properties was use a complex dielectric function $\varepsilon(\hbar\omega)$. Using Kramers–Kronig relation was calculation refractive index. The maximum value of the refractive index for solid-state $Cd_{0.75}X_{0.25}Te$ solutions was obtained for *X*= Au near 435 nm.

Acknowledgments

This work was supported by the Project of Young Scientists 0121U108649 of the Ministry of Education and Science of Ukraine.

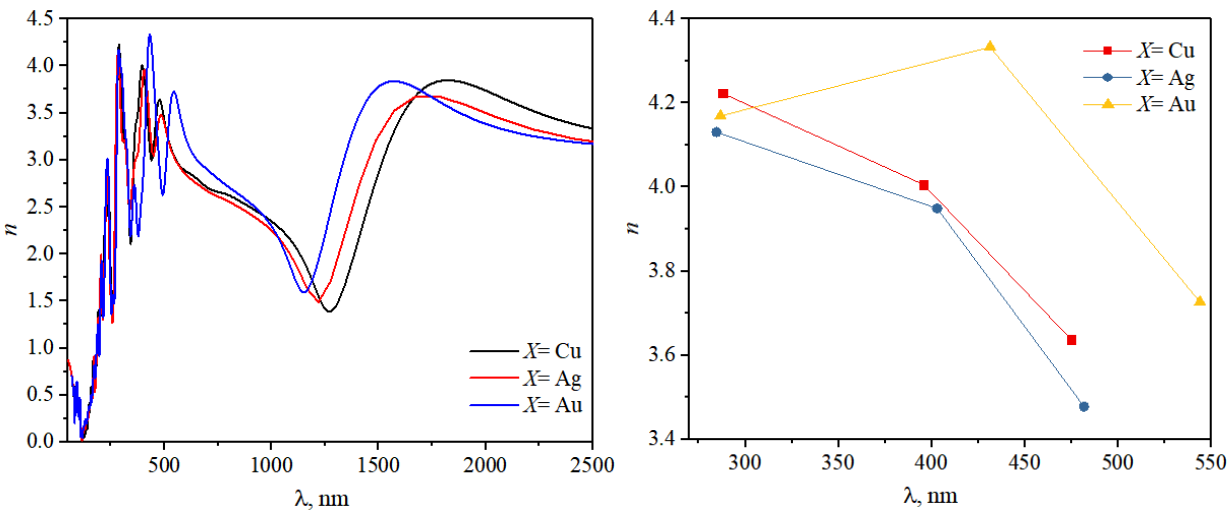

Fig. 9. Spectral behaviour of the refractive index (*a*) of solid-state $Cd_{0.75}X_{0.25}Te$ (*X*= Cu, Ag and Au) solutions (see information in legend). The three maximum values of the refractive index for the visible spectral region (*b*).

Kashuba A.I. – Ph.D, Doctoral Student at the Department of General Physics;.

[1] A. Kashuba, I. Semkiv, O. Kushnir, *Basic physical properties of thin films of cadmium chalcogenides*, LAP Lambert Academic Publishing, Riga, Latvia 2021.
[2] R. Petrus, H. Ilchuk, A. Kashuba, I. Semkiv, E. Zmiiovska, *Optical properties of CdTe thin films obtained by the method of high-frequency magnetron sputtering*, Functional Materials, 27(2), 342 (2020); https://doi.org/10.15407/fm27.02.342.
[3] Z.R. Zapukhlyak, L.I. Nykyruy, V.M. Rubish,G. Wisz, V.V. Prokopiv, M.O. Galushchak, I.M. Lishchynskyy, L.O. Katanova, R.S. Yavorskyi, *SCAPS simulation of ZnO/CdS/CdTe/CuO heterostructure for photovoltaic application*, Physics and Chemistry of Solid State, 21(4), 660 (2020); https://doi.org/10.15330/PCSS.21.4.660-668.
[4] H. Ilchuk, R. Petrus, I. Semkiv, A. Kashuba, *Directional Synthesis of CdX (X = S, Se, and Te) Thin Films for Solar Cell Application*, Springer Proceedings in Physics, 247, 117 (2020). https://doi.org/10.1007/978-3-030-52268-1_9.
[5] T. Saga, *Advances in Crystalline Silicon Solar Cell Technology for Industrial Mass Production*, NPG Asia Materials, 2, 96 (2010); http://dx.doi.org/10.1038/asiamat.2010.82.
[6] Z. Bai, J. Yang, D. Wang, *Thin film CdTe solar cells with an absorber layer thickness in micro- and sub-micrometer scale*, Appl. Phys. Lett. 99, 143502 (2011);. https://doi.org/10.1063/1.3644160.
[7] Y. Deng, J. Yang, R. Yang, K. Shen, D. Wang, D. Wang, *Cu-doped CdS and its application in CdTe thin film solar cell*, AIP ADVANCES, 6, 015203 (2016); https://doi.org/10.1063/1.4939817.
[8] J.L. Freeouf, J.M. Woodall, *Schottky barriers: An effective work function model*, Appl. Phys. Lett., 39, 727 (1981); https://doi.org/10.1063/1.92863.
[9] S.H. Demtsu, J.R. Sites, *Effect of back-contact barrier on thin-film CdTe solar cells*, Thin Solid Films, 510, 320 (2006); https://doi.org/10.1016/j.tsf.2006.01.004.
[10] A. Bosioa, R. Ciprian, A. Lamperti, I. Rago, B. Ressel, G. Rosa, M. Stupar, E. Weschke, *Interface phenomena between CdTe and ZnTe:Cu back contact*, Solar Energy, 176, 186 (2018); https://doi.org/10.1016/j.solener.2018.10.035.
[11] K.A. Aris, K.S. Rahman, A.M. Ali, B. Bais, I.B. Yahya, Md. Akhtaruzzaman, H. Misran, S.F. Abdullah, M.A. Alghoul, N.Amin, *A comparative study on thermally and laser annealed copper and silver doped CdTe thin film solar cells*, Solar Energy, 173, 1 (2018). https://doi.org/10.1016/j.solener.2018.07.009.
[12] T.D. Dzhafarov, S.S. Yesilkaya, N.Y. Canli, M. Caliskan, *Diffusion and influence of Cu on properties of CdTe thin films and CdTe/CdS cells*, Solar Energy Materials & Solar Cells, 85, 371 (2005);https://doi.org/0.1016/j.solmat.2004.05.007.
[13] T.A. Gessert, A.R. Mason, P. Sheldon, A.B. Swartzlander, D. Niles, T.J. Coutts, *Development of Cu-doped ZnTe as a back-contact interface layer for thin-film CdS/CdTe solar cells*, J. Vac. Sci. Technol. A, 14(3), 806 (1996); http://dx.doi.org/10.1116/1.580394.
[14] D. Grecu, A.D. Compaan, D. Young, U. Jayamaha, D.H. Rose, *Photoluminescence of Cu-doped CdTe and related stability issues in CdS/CdTe solar cells*, Journal of Applied Physics, 88, 2490 (2000); http://dx.doi.org/10.1063/1.1287414.
[15] J. Perrenoud, L. Kranz, C. Gretener, F. Pianezzi, S. Nishiwaki, S. Buecheler, A.N. Tiwari, *A comprehensive picture of Cu doping in CdTe solar cells*, Journal of Applied Physics, 114, 174505 (2013); http://dx.doi.org/10.1063/1.4828484.
[16] G.H. Tariq, M. Anis-ur-Rehman, *Annealing effects on physical properties of doped CdTe thin films for photovoltaic applications*, Materials Sciencein Semiconductor Processing, 30, 665 (2015); https://doi.org/10.1016/j.mssp.2014.09.012
[17] H.H. Woodbury, M. Aven, *Some Diffusion and Solubility Measurements of Cu in CdTe*, Journal of Applied Physics, 39, 5485 (1968); http://dx.doi.org/10.1063/1.1655999.
[18] J.P. Chamonal, E. Molva, J.L. Pautrat, *Identification of Cu and Ag acceptors in CdTe*, Solid State Communications, 43(1l), 801 (1982); https://doi.org/10.1016/0038-1098(82)90843-2.
[19] V. Dzhagan, O. Kapush, O. Isaieva, S. Budzulyak, O. Magda, P.P. Kogutyuk, L. Trishchuk, V. Yefanov, M. Valakh, V. Yukhymchuk, *Tuning the photoluminescence of CdTe quantum dots by controllable coupling to plasmonic Au nanoparticles*, Physics and Chemistry of Solid State, 23(4), 720 (2022); https://doi.org/10.15330/pcss.23.4.720-727.
[20] V. Lesnyak, A. Wolf, A. Dubavik, L. Borchardt, S.V. Voitekhovich, N. Gaponik, S. Kaskel, A. Eychmuller, *3D Assembly of Semiconductor and Metal Nanocrystals: Hybrid CdTe/Au Structures with Controlled Content*, J. Am. Chem. Soc., 133, 13413 (2011); http://dx.doi.org/10.1021/ja202068s.
[21] I. Bouziani, Y. Benhouria, I. Essaoudi, A. Ainane, R. Ahuja, *Magnetoelectronic properties of Vanadium impurities co-doped (Cd, Cr)Te compound for spintronic devices: First principles calculations and Monte Carlo simulation*, Journal of Magnetism and Magnetic Materials, 466, 420 (2018); https://doi.org/10.1016/j.jmmm.2018.07.033.

[22] N.A. Noor, S. Ali, A. Shaukat, *First principles study of half-metallic ferromagnetism in Cr-doped CdTe*, Journal of Physics and Chemistry of Solids, 72, 836 (2011); https://doi.org/10.1016/j.jpcs.2011.04.008.
[23] K.L. Yao, G.Y. Gao, Z.L. Liu, L. Zhu, Y.L. Li, *Half-metallic ferromagnetic semiconductors of V- and Cr-doped CdTe studied from first-principles pseudopotential calculations*, Physica B, 366, 62 (2005); https://doi.org/10.1016/j.physb.2005.05.024.
[24] M.A. Flores, E. Menéndez-Proupin, W. Orellana, J.L. Peña, *Sn-doped CdTe as promising intermediate-band photovoltaic material*, J. Phys. D: Appl. Phys., 50, 035501 (2017); https://doi.org/10.1088/1361-6463/50/3/035501.
[25] F. Goumrhar, L. Bahmad, O. Mounkachi, A. Benyoussef, *Calculated magnetic properties of co-doped CdTe (V,P): First-principles calculation,* Computational Condensed Matter., 13, 87 (2017); https://doi.org/10.1016/j.cocom.2017.09.009.
[26] Jie Ma, Su-Huai Wei, T.A. Gessert, K.K. Chin, *Carrier density and compensation in semiconductors with multiple dopants and multiple transition energy levels: Case of Cu impurities in CdTe*, Physical Review B, 83, 245207 (2011); https://doi.org/10.1103/PhysRevB.83.245207.
[27] M. Sajjad, H.X. Zhang, N.A. Noor, S.M. Alay-e-Abbas, A. Shaukat, Q. Mahmood, *Study of half-metallic ferromagnetism in V-doped CdTe alloys by using first-principles calculations*, Journal of Magnetism and Magnetic Materials, 343, 177 (2013); http://dx.doi.org/10.1016/j.jmmm.2013.04.045.
[28] J.-H. Yang, W.-J. Yin, J.-S. Park, J. Burst, W.K. Metzger, T. Gessert, T. Barnes, S.-H. Wei, *Enhanced p-type dopability of P and As in CdTe using non-equilibrium thermal processing*, Journal of Applied Physics, 118, 025102 (2015); http://dx.doi.org/10.1063/1.4926748.
[29] H. Zhu, M. Gu, L. Huang, J. Wang, X. Wu, *Structural and electronic properties of CdTe:Cl from first-principles*, Materials Chemistry and Physics, 143, 637–641 (2014); http://dx.doi.org/10.1016/j.matchemphys.2013.09.046.
[30] R.Yu. Petrus, H.A. Ilchuk, V.M. Sklyarchuk, A.I. Kashuba, I.V. Semkiv, E.O. Zmiiovska, *Transformation of Band Energy Structure of Solid Solutions CdMnTe*, J. Nano- Electron. Phys., 10(6), 06042-1 (2018); https://doi.org/10.21272/jnep.10(6).06042.
[31] H. Ilchuk, E. Zmiiovska, R. Petrus, I. Semkiv, I. Lopatynskyi, A. Kashuba, *Optical Properties of CdMnTe Film: Experimental and Theoretical Aspects*, Journal of Nano- and Electronic Physics, 12(1), 01027-1 (2020); https://doi.org/ 10.21272/jnep.12(1).01027.
[32] Q. Mahmood, M. Hassan, *Systematic first principle study of physical properties of Cd0.75Ti0.25Z (Z = S, Se,Te) magnetic semiconductors using mBJ functional*, Journal of Alloys and Compounds, 704, 659 (2017); https://doi.org/10.1016/j.jallcom.2017.02.097.
[33] M.H. Tedjini, A. Oukebdane, M.N. Belkaid, N. Aouail, *The effect of zinc concentration upon electronic structure, optical and dielectric properties of Cd1− xZnxTe alloy: TB-mBJ investigation*, Computational Condensed Matter., 27, e00561 (2021); https://doi.org/10.1016/j.cocom.2021.e00561.
[34] J.L. Roehl, S.V. Khare, *Diffusion of Cd vacancy and interstitials of Cd, Cu, Ag, Au and Mo in CdTe: A first principles investigation*, Solar Energy. 101, 245 (2014); http://dx.doi.org/10.1016/j.solener.2013.12.017.
[35] H.A. Ilchuk, L.I. Nykyruy, A.I. Kashuba, I.V. Semkiv, M.V. Solovyov, B.P. Naidych, V.M. Kordan, L.R. Deva, M.S. Karkulovska, R.Y. Petrus, *Electron, Phonon, Optical and Thermodynamic Properties of CdTe Crystal Calculated by DFT*, Physics and Chemistry of Solid State, 23(2), 261 (2022); https://doi.org/10.15330/pcss.23.2.261-269.
[36] J.P. Perdew, K. Burke, and M. Ernzerhof, *Generalized Gradient Approximation Made Simple*, Phys. Rev. Lett., 78(7), 1396 (1997); https://doi.org/10.1103/PhysRevLett.78.1396).
[37] H.J. Monkhorst and J.D. Pack, *Special Points for Brillouin-Zone Integrations*, Phys. Rev. B., 13(12), 5188 (1976); https://doi.org/10.1103/PhysRevB.13.5188.
[38] W. Kohn and L. J. Sham, *Self-Consistent Equations Including Exchange and Correlation Effects*, Phys. Rev. A., 140(4), 1133 (1965); https://doi.org/10.1103/PhysRev.140.A1133.
[39] M. Kovalenko, O. Bovgyra, V. Dzikovskyi, R. Bovhyra, *DFT study for adsorption of CO and H2 on Pt-doped ZnO nanocluster*, SN Appl. Sci. 2, 790 (2020); https://doi.org/10.1007/s42452-020-2591-9.
[40] C. Wang, J. Bernholc, R.F. Davis, *Formation energies, abundances, and the electronic structure of native defects in cubic SiC*, Phys. Rev. B, 38, 12752(R) (1988); https://doi.org/10.1103/PhysRevB.38.12752.
[41] A. Kashuba, B. Andriyevskyy, I. Semkiv, L. Andriyevska, R. Petrus, E. Zmiiovska, D. Popovych, *Influence of Defective Formations on Photoconductivity of Layered Crystals with Cationic Substitution*, Journal of Nano- and Electronic Physics, 10(6), 06025 (2018); https://doi.org/10.21272/jnep.10(6).06025.
[42] A. Fonari, C. Sutton, Effective Mass Calculator (2012). https:// github. com/ afona ri/ emc.
[43] M. Aven, J. Prener, Physics and Chemistry of II-VI Compounds, John Wiley and Sons, New York, 1967.
[44] Z. Yinnü, Y. Jinliang, X. Chengyang, *First-principles study on electronic structure and conductivity of Sn-doped* $Ga_{1.375}In_{0.625}O_3$, Journal of Semiconductors, 36, 012003 (2015); https://doi.org/10.1088/1674-4926/36/1/012003.
[45] J. Liu, Q.-Y. Jiang, S.-D. Zhang, H. Zhang, *Carrier mobility and relaxation time in BiCuSeO*, Physics Letters A, 383, 125990 (2019); https://doi.org/10.1016/j.physleta.2019.125990.

А.І. Кашуба

Вплив заміщення атомів металу на електронні та оптичні властивості твердих розчинів $Cd_{0.75}X_{0.25}Te$ (*X*= Cu, Ag та Au)

Кафедра загальної фізики, Національний університет "Львівська політехніка", Львів, Україна, andrii.i.kashuba@lpnu.ua

Тверді розчини $Cd_{0.75}X_{0.25}Te$ (*X*= Cu, Ag і Au), кристалізовані в кубічній структурі, досліджуються в рамках теорії функціоналу густини. Розрахунки з перших принципів електронної зонної структури, густини станів і показника заломлення твердих розчинів $Cd_{0.75}X_{0.25}Te$ (*X*= Cu, Ag і Au) оцінені за допомогою узагальненого градієнтного наближення (GGA). Було використано функціонал Пердью–Берка–Ернзерхофа (PBE). Енергія утворення розрахована за результатами загальної енергії досліджуваних зразків. На основі електронної зонної структури було розраховано ефективну масу електронів і дірок. Обговорено вплив заміщення атомів на електронну провідність і рухливість. Для дослідження оптичних властивостей використовували комплексну діелектричну функцію ε(ħω). Спектральна поведінка показника заломлення була розрахована на основі діелектричної функції.

Ключові слова: теорія функціонала густини, електронна енергетична структура, енергія формування, ефективна маса, щільність станів, показник заломлення.